frontiers in Materials

ORIGINAL RESEARCH
published: 03 February 2022
doi: 10.3389/fmats.2022.824364

The Innovative Self-Sensing Strain Sensor for Asphalt Pavement Structure: Substitutability and Synergy Effects of Graphene Platelets With Carbon Nanotubes in Epoxy Composites

Xue Xin[1], Xuehao Luan[1], Linping Su[1], Chuanyi Ma[2], Ming Liang[1], Ximao Ding[3] and Zhanyong Yao[1]**

[1]School of Qilu Transportation, Shandong University, Jinan, China, [2]Shandong HI-SPEED Group, Jinan, China, [3]Shandong HI-SPEED Jiwei Expressway Co., Ltd., Jinan, China

OPEN ACCESS

Edited by:
Han-Cheng Dan,
Central South University, China

Reviewed by:
Huaping Wang,
Lanzhou University, China
Ping Xiang,
Central South University, China

***Correspondence:**
Ming Liang
ming.liang@sdu.edu.cn
Zhanyong Yao
zhanyong-y@sdu.edu.cn

Specialty section:
This article was submitted to Structural Materials, a section of the journal Frontiers in Materials

Received: 29 November 2021
Accepted: 03 January 2022
Published: 03 February 2022

Citation:
Xin X, Luan X, Su L, Ma C, Liang M, Ding X and Yao Z (2022) The Innovative Self-Sensing Strain Sensor for Asphalt Pavement Structure: Substitutability and Synergy Effects of Graphene Platelets With Carbon Nanotubes in Epoxy Composites. Front. Mater. 9:824364. doi: 10.3389/fmats.2022.824364

Situ sensors with high accuracy, long durability, and high survival rate are crucial for the health monitoring of asphalt pavement. Due to the harsh environment during the construction period and service life, the monitoring components which can be buried synchronously with the construction period of the road surface become a difficult problem to be solved urgently. The development of functional composites sheds a new insight for pavement strain detection with remarkable self-sensing behavior. In this paper, the substitutability and synergy effect of graphene platelets with carbon nanotubes (CNTs), the effect of CNT types with different specific surface areas in epoxy composites to the morphological, electrical, and mechanical properties, and the strain-electrical resistance response peculiarity of composites were evaluated. The performance of developed composite sensors with epoxy encapsulation was investigated through laboratory experiments. The morphologies showed that CNT-GNP hybrids in composites present a better dispersion state because of the size effect and synergetic effect whereas the pure CNTs are prone to entangle with each other. Composites with CNT(SSA500) display the most amounts of conductive units in same dosage. CNTs and GNP can strengthen the elastic modulus of the epoxy matrix to basically the same as that of asphalt mixture within the range of 1100–1500 MPa. At last, Laboratory experiments have proved the promising prospect for CNTs-GNP/epoxy composites serving as the strain sensor. The developed composites-based strain sensor can provide a new prospect for asphalt pavement monitoring.

Keywords: self-sensing property, asphalt pavement structure, strain sensor, composites, substitutability and synergy effects

INTRODUCTION

With the development of road construction and design, asphalt pavement is supposed to be an intelligent infrastructure with properties of intelligence, automation, and informatization (Ko and Ni, 2005; Abdo, 2014). As the important development direction and basic elements for the intelligent road, the sensing network should be endowed with the abilities of active perception (Soong and Cimellaro, 2009; Ku-Herrera et al., 2016; Sony et al., 2019). It is regarded that keeping the health monitoring abreast with the pavement construction and service period among the whole life cycle are crucial for the design, maintenance management, and assessment. In general, the strain of asphalt pavement structure is much smaller within hundreds or even ten times the micro strain. Therefore, situ sensors with good monitoring accuracy, long durability, and high survival rate are very important for asphalt pavement. In recent years, the optical fibre-based sensors for strain monitoring of asphalt pavement has attracted the attention of many scholars. The transverse and longitudinal directions and distresses, such as cracks, ruts, and settlements can be efficiently measured by distributed optical fibre sensing technology (Xiang and Wang, 2016; Wang et al., 2018; Xiang and Wang, 2018; Wang et al., 2020). However, with the effect of complex construction conditions, such as heavy compaction and high-temperature of asphalt concrete, heavy vehicles, and extreme environments over its life-span, the traditional strain sensors are usually difficult to maintain in the asphalt pavement structure (Hasni et al., 2017; Escalona-Galvis and Venkataraman, 2021). Besides, the poor durability and deformation incompatibility of conventional sensing elements also restrict the development of intelligent monitoring for road engineering. Moreover, the insufficient service period is much less than the designed life of the road, further resulting in high maintenance costs (Cheng and Miyojim, 1998; Dai, 2017; Han et al., 2020).

In recent years, the development of composites sheds new insight on the strain detection of pavement (Li et al., 2004; Gao et al., 2009; Hu et al., 2010; Eswaraiah et al., 2012; Xi and Chung, 2020). With the remarkable self-sensing and special functional ability, composite smart materials are responsive to the effect of deformation, force, or other factors (Xi and Chung, 2020; Yang et al., 2021). Application of self-sensing composites in the field of civil engineering can mainly be divided into two categories based on the matrix materials, one is the common civil engineering materials of cement or asphalt and the other is polymer (Thostenson and Chou, 2006; Wang et al., 2015; Can-Ortiz et al., 2019). Considering the advantages of high reactivity and controllable mechanical properties, epoxy resins are widely used in the composites. Conducting materials in the composites play a vital role for the self-sensing characteristics with the electrical signal sensitivity peculiarity as the deformation of composite materials (Xin et al., 2022). Among the diverse conductive materials, carbon materials such as carbon nanotubes (CNTs), carbon blacks (CB), graphenes (GNPs), and carbon fibers have been the predominant conductive materials due to the good conductivity and mechanical properties (Li et al., 2018; Park et al., 2020). The conductive fillers are dispersed in the polymer matrix and can form a conductive system. The optimizations of conducting systems and accurate evaluation of composites' properties have attracted considerable interest from researchers (Chen et al., 2007; Han et al., 2009; Campo et al., 2015; Bisht et al., 2020; Koo and Tallman, 2020). In our previous studies, the aligned multiwall carbon nanotubes with excellent electrical conductivity were used to prepare the epoxy matrix composites for a novel strain sensor, which can effectively monitor the micro-strain in the field of road engineering (Xin et al., 2020). CNTs exhibit excellent mechanical, electrical, and thermodynamic properties due to the special volume effect, tunneling effect, and size effect, which makes the development and innovation of micro-strain sensor possible (Li et al., 2004; Gao et al., 2009; Chung, 2012). However, it is generally acknowledged that the combination of more than one filler can improve the electrical properties or mechanical properties for the composites because of the synergistic effect (Wei et al., 2010). Some studies investigated the influence of two or three fillers on the mechanical, electrical, or morphological behavior of polymers. Li et al. (Li et al., 2013a) developed the hybrid fillers composed of CNTs grown on GNPs and dispersed them into epoxy matrix. They presented that the embedding of CNT–GNP hybrids into pristine epoxy endows optimum dispersion of CNTs and GNPs as well as better interfacial adhesion between the carbon fillers and matrix, which results in a significant improvement in load transfer effectiveness. I. Kranauskaite et al. (Kranauskaitė et al., 2018) investigated the enhancing electrical conductivity of CNTs/epoxy composites by mixing the GNPs at a fixed content of 0.3 wt%. They found that the mixed particles did not interfere with the percolative behavior of CNTs but can improve the overall electrical performances. Jan Sumfleth et al. (Sumfleth et al., 2011) evaluated the comparison of rheological and electrical percolation phenomena in carbon black and carbon nanotube filled epoxy polymers, which demonstrated that the differences between the rheological and electrical percolation thresholds are dependent on the curing conditions. These interesting works have proved the advantages of hybrids fillers. But few studies have been carried out to introduce the self-sensing properties at such a small micro-strain range as the *in situ* sensor. The substitution effects of GNP with CNTs by the same content have not been investigated in detail. Moreover, most researchers have mainly focused on the properties of composite materials, but have not taken the engineering applications into consideration.

In the present research, the developed strain sensors based on CNT-GNP hybrids/epoxy composites were investigated. The influences of CNTs types with different aspect ratios/specific surface areas (SSA) on the CNT-GNP hybrids/epoxy composites were evaluated simultaneously (Li et al., 2013b; Zakaria et al., 2017). Based on ultrasonic dispersion and micro-nano conducting structure analysis, the dispersion behavior of CNT-GNP hybrids in epoxy resin and its influence to the electrical, mechanical properties, and strain-electrical resistance response peculiarity of composites were respectively analyzed. In addition, with the aims of ultra-high detection accuracy and micro-strain sensitivity for the pavement applications, the self-sensing composite materials were

TABLE 1 | Basic information of CNTs with different SSA and laminar GNP.

	CNT(SSA165)	CNT(SSA500)	CNT(SSA60)	Laminar GNP	
Purity (wt%)	95	>98	98	D50 diameter (um)	7~10
Out Diameter (nm)	10–20	4~6	>50	Stacking density (g/ml)	0.08~0.13
Length (μm)	50–100	10–20	<15	Tablet resistance (mΩ·cm)	5.6
Special surface area (m^2/g)	165	~500	>60	Carbon content (wt%)	>98
Electric Conductivity (s/cm)	>100	>100	>100		
ASH (wt%)	<5	<1.5	<5		

conducted with encapsulation and formed the studied process. At last, the sensor installed with the specific T-shaped aluminum structure was subjected to the asphalt mixture experiment to simulate the pavement environment and verify the applicability.

EXPERIMENTAL

Materials

The polymer matrix used in this study is thermosetting epoxy resin compounded by bisphenol A and epichlorohydrin, which have the advantages of high reactivity and controllable mechanical properties. The epoxy resin and polyamide curing agent were achieved commercially (Xingcheng Co.Ltd., Nantong, China and Xiangshan Company, Beijing, China) and matched in a mass ratio of 100:30. Three types of CNTs with different SSA and the laminar GNP were supplied by JCNANO Technology Company, China. The basic information of the conducting carbon fillers are summarized in **Table 1**.

Preparation of the Composites

Three types of CNTs with different special surface areas and laminar GNPs of specific mass were grinded and dispersed respectively in the N, N-dimethyl -formamide (DMF) using mechanical agitation with 300 rpm for 10 min and ultrasonic instrument (UH450, Oulior) with 5 s ON and 3 s OFF cycle for 10 min. Then the CNTs suspension and the laminar GNP suspension were blended and sonicated for 20 min. The two steps were performed to obtain the uniform fillers suspensions. Considering the CNTs size of nanoscale and the GNP size of microscale, the dispersion degree of CNT-GNP will directly determine the conductive behavior of the composites, the preparation of suspension is the crucial step. After that, epoxy resin was poured into the blended suspensions along the container wall for minimizing the introduction of bubbles. Then the samples were stirred mechanically for 30 min at 1000 rpm and sonicated for 90 min. What calls for special attention is that the mixture of epoxy resin and suspensions presents high viscosity during sonicating, so stirring was conducted at the same time while sonicating to ensure the effective dispersion of the conductive fillers. Furthermore, the samples were maintained with water cooling so as to prevent a temperature rise in the ultrasonic state, which may lead to the aggregation of conductive fillers. The mixture was then conducted in the vacuum drying oven at 80°C for 60 min to eliminate the DMF solvent completely. After cooling down to room temperature, polyamide curing agent was added into the samples and stirred mechanically for 10 min at 300 rpm. Then the produced composites were poured into the dumbbell-shaped polytetrafluoroethylene mold and the self-developed silicone tube mold. After being cured at room temperature for 24 h and 80°C for 2 h, samples were de-molded and further cured at 120°C for 4 h. The schematic of **Figure 1** shows the preparation process of the epoxy composites. Descriptions of the compositions of samples in naming are listed in **Table 2**. The CNTs were partially substituting by GNP at same dosage.

Characterizations

Morphology

The morphologies of CNT(SSA165), CNT(SSA500), CNT(SSA60), and laminar GNP were observed by the scanning electron microscopy (SEM, Hitachi SU8010). Powders of three CNTs with different special surface areas and GNP were treated by oven drying and spray-gold and observed under an accelerating voltage of 10 KV. The SEM for the fractured surfaces of the 12 epoxy composites samples were all conducted, in order to illuminate conductive structure formed by the CNTs and GNP and the interfacial interaction between the epoxy and carbon fillers. Combining with the morphologies, the electrical conductivity, strain-electrical resistance response and toughening mechanism of the epoxy composites can be analyzed and verified deeply.

Electrical Conductivity and Strain-Electrical Resistance Response

The electrical conductivity of epoxy composites was measured by the digital voltage-current meter of Keithley DAQ 6510 with the maximum resistance range of 100 MΩ using a two-probe method. Wires were embedded into the composites directly by the self-developed silicone tube mold, which will be introduced in detail in *Sensor Encapsulation and Bending Strain Test in Asphalt Concrete Beam Section*. Data of electrical resistance R can be acquired directly from the instrument and the electrical conductivity ρ can be calculated by the formula of $\rho = \frac{RS}{L}$, where S and L are the cross sectional area and length of composites sample, respectively. In the present study, the samples were prepared with 4 mm in diameter and 100 mm in length. All the electrical conductivity data are the average of three measurements.

Strain-electrical resistance response was measured using a self-developed test system, see **Figure 2**. Differing from other research, the test system was specially designed for obtaining

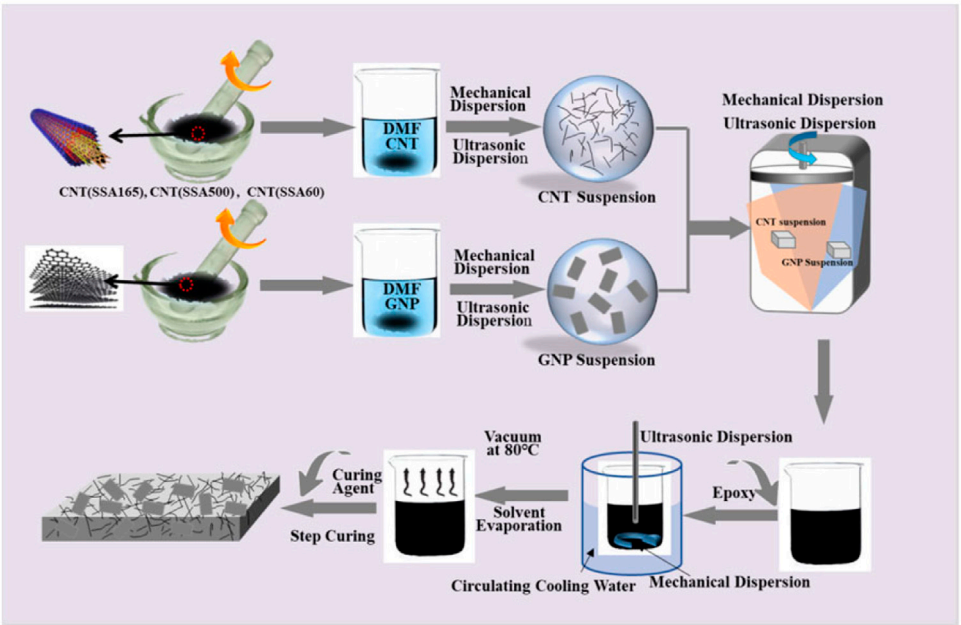

FIGURE 1 | Preparation process schematic of the composites for asphalt pavement strain monitoring.

TABLE 2 | Descriptions of the compositions samples in naming.

Epoxy composites	Descriptions
$CNT(SSA165)_{0.8}$/EP	Epoxy filled with 0.8 wt% CNT(SSA165)
$CNT(SSA165)_{0.7}GNP_{0.1}$/EP	Epoxy filled with 0.7 wt% CNT(SSA165) and 0.1 wt% GNP
$CNT(SSA165)_{0.6}GNP_{0.2}$/EP	Epoxy filled with 0.6 wt% CNT(SSA165) and 0.2 wt% GNP
$CNT(SSA165)_{0.5}GNP_{0.3}$/EP	Epoxy filled with 0.5 wt% CNT(SSA165) and 0.3 wt% GNP
$CNT(SSA500)_{0.8}$/EP	Epoxy filled with 0.8 wt% CNT(SSA500)
$CNT(SSA500)_{0.7}GNP_{0.1}$/EP	Epoxy filled with 0.7 wt% CNT(SSA500) and 0.1 wt% GNP
$CNT(SSA500)_{0.6}GNP_{0.2}$/EP	Epoxy filled with 0.6 wt% CNT(SSA500) and 0.2 wt% GNP
$CNT(SSA500)_{0.5}GNP_{0.3}$/EP	Epoxy filled with 0.5 wt% CNT(SSA500) and 0.3 wt% GNP
$CNT(SSA60)_{0.8}$/EP	Epoxy filled with 0.8 wt% CNT(SSA60)
$CNT(SSA60)_{0.7}GNP_{0.1}$/EP	Epoxy filled with 0.7 wt% CNT(SSA60) and 0.1 wt% GNP
$CNT(SSA60)_{0.6}GNP_{0.2}$/EP	Epoxy filled with 0.6 wt% CNT(SSA60) and 0.2 wt% GNP
$CNT(SSA60)_{0.5}GNP_{0.3}$/EP	Epoxy filled with 0.5 wt% CNT(SSA60) and 0.3 wt% GNP

the accurate micro-strain with the scale less than 100 με, which is the general strain range in asphalt pavement. With the samples clamping fixed on the strain control device (see **Figure 2A**), the variation of strain will be measured by the strain extensometer and displayed in the PC interface when rotating the hand wheel. At the same time, the electrical resistance R is automatically recorded by Keithley DAQ 6510 and illustrated in another PC interface. The parameter of resistance variation rate can be calculated by $\triangle R/R_0 = (R-R_0)/R_0*100\%$.

Mechanical Property

Dumbbell-shaped epoxy composites samples were prepared with the PVDF molds. The quasi-static tensile tests were conducted in the universal testing machine of SANS at room temperature. Direct tensile test loaded with a constant displacement rate of 0.2 mm/min until the samples were broken. The strain-stress curves, mechanical property parameters of tensile elastic modulus, elongation at break, and breaking strength can be obtained from the direct tensile test. Three replicates for one sample were measured to obtain the average value of mechanical property parameters.

RESULTS AND DISCUSSION

SEM Morphology of Carbon Fillers and Composites

SEM images of the three types of CNTs with different special surface areas (SSA) of CNT (SSA165), CNT (SSA500), CNT (SSA60), and GNP are shown in **Figure 3**. SSA are defined as the total area (S) of the CNTs per unit mass (m), i.e., SSA = S/m or can be calculated by the formula of SSA = S/V, in which S means

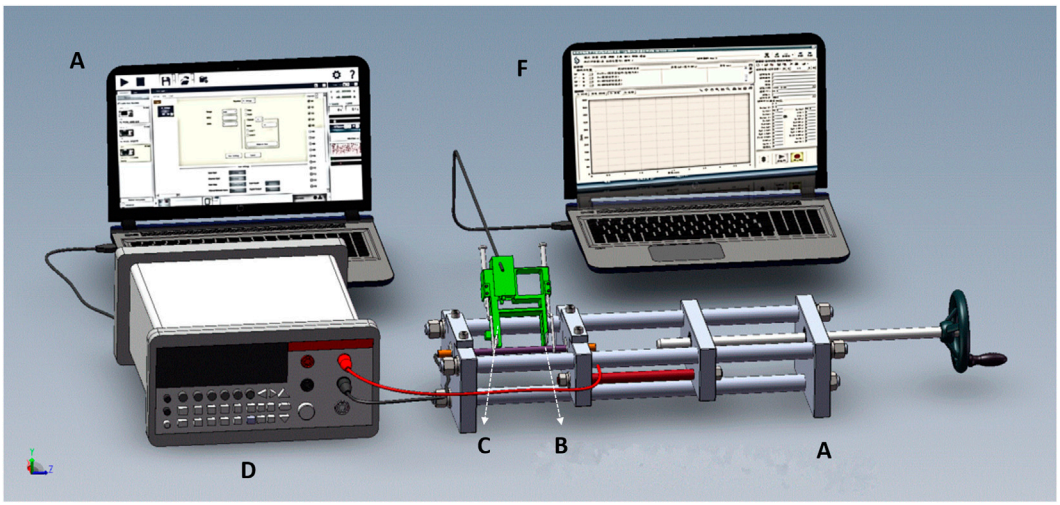

FIGURE 2 | Self-developed test system for strain-electrical resistance response, **(A)** Strain control device, **(B)** Specimen, **(C)** Extensometer, **(D)** Digital multimeter, **(E, F)** data record computer.

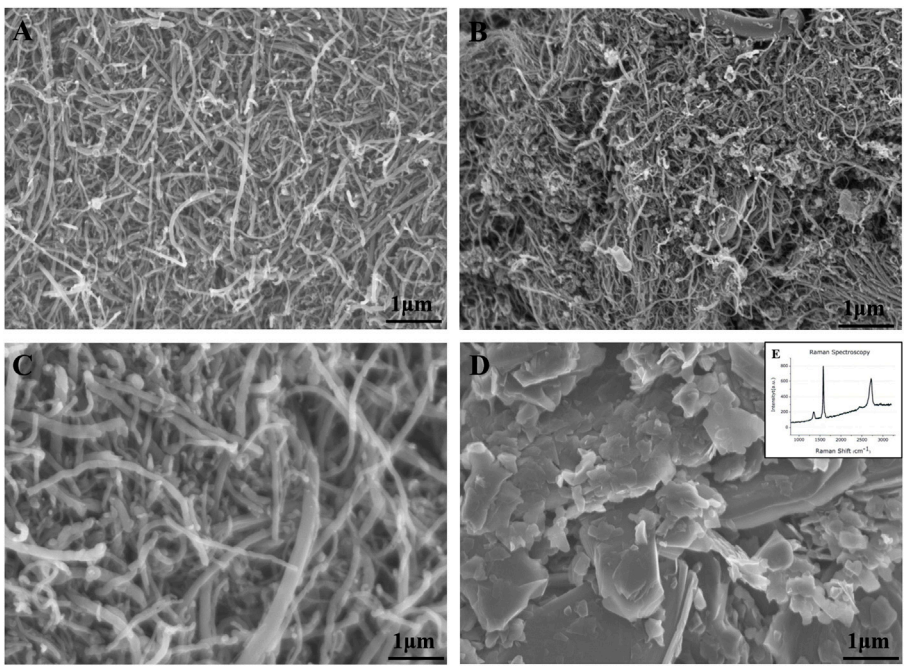

FIGURE 3 | SEM images of **(A)** CNT (SSA165), **(B)** CNT (SSA500), **(C)** CNT (SSA60), **(D)** GNP.

the total area, V means the volume of CNTs. It can be seen that the tortuous and sinuate CNTs entangled with each other because of the elongated tubular structure and strong Van der Waals forces. Furthermore, the entanglement degree appears much more tightly with the higher SSA, seen in **Figure 2B**. However, the larger the value of SSA, the more carbon nanotubes per unit volume. Thus, the total interface area with the epoxy resin matrix will decline sharply in the composites. On the other hand, the surface of the CNTs is hydrophobic and CNTs tend to aggregate into bundles in solution. Based on this, it is crucial to disperse CNTs in the epoxy resin matrix effectively and uniformly, in order to optimize the mechanical and electrical

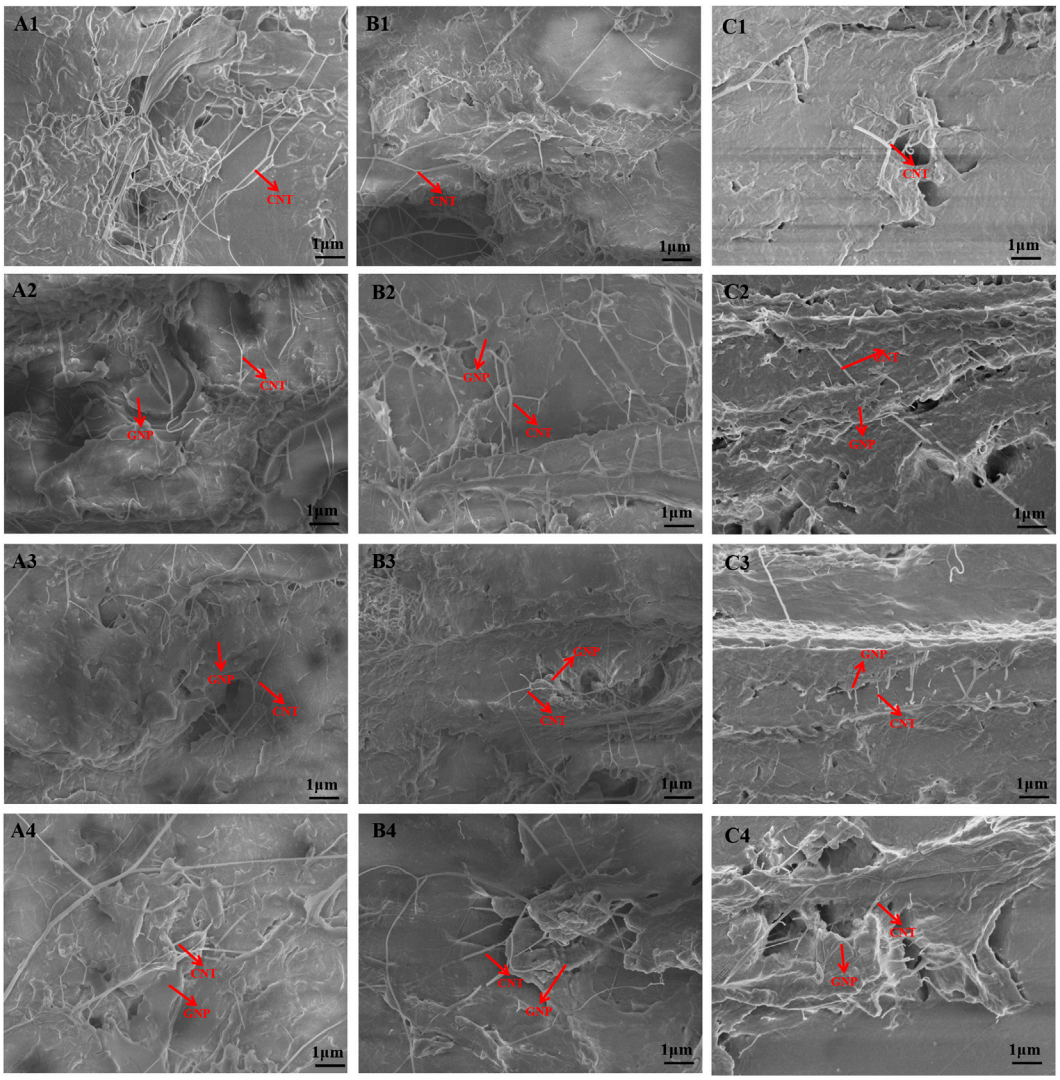

FIGURE 4 | SEM of the fracture surfaces for epoxy composites with different fillers, **(A1)** CNT(SSA165)0.8/EP, **(A2)** CNT(SSA165)$_{0.7}$GNP$_{0.1}$/EP, **(A3)** CNT(SSA165)$_{0.6}$GNP$_{0.2}$/EP, **(A4)** CNT(SSA165)0.5GNP0.3/EP, **(B1)** CNT(SSA500)0.8/EP, **(B2)** CNT(SSA500)0.7GNP0.1/EP, **(B3)** CNT(SSA500)0.6GNP0.2/EP, **(B4)** CNT(SSA500)0.5GNP0.3/EP, **(C1)** CNT(SSA60)0.8/EP, **(C2)** CNT(SSA60)0.7GNP0.1/EP, **(C3)** CNT(SSA60)0.6GNP0.2/EP, **(C4)** CNT(SSA60)0.5GNP0.3/EP.

performance and prevent the stress concentration areas. Similar viewpoints were also reported in previous studies (Liu et al., 2017; Liu and An, 2018; Han et al., 2019). Considerable interests have been put forward by modifying the CNTs structure or introducing other fillers to promote the dispersion and directional arrangement. **Figure 3D** demonstrates the SEM image of the GNP. The GNP displays laminar and plate-like structure and the size of sheet varies. The sheet of GNP shows a coarse surface, so it is expected to be beneficial in connecting with the CNTs.

SEM morphologies of the fracture surfaces of CNT/GNP/EP composites were investigated to measure the dispersion of CNTs-GNP fillers (displayed in **Figure 4**). It can be seen that a CNT-GNP hybrid (see **Figures 4A2–C4**) shows a better dispersion state (Li et al., 2013b; Xi and Chung, 2020). Unlike the pure CNTs which are entangled with each other, most of the CNTs are well dispersed in the composites in the presence of GNP and ultrasonication. The previous tortuous CNTs are separated individually and formed directional alignment in the composites. In the case of a CNT-GNP hybrid conductive structure, CNTs are arranged among the adjacently laminar GNP and the original configuration of pure CNTs or GNP are disrupted and rearranged. In most instances, the CNTs or GNP tend to aggregate because of the high Van der Waals forces (Thostenson and Chou, 2006). However, when the GNP was introduced into the composites, CNTs in nano scale are easily prone to be dispersed homogenously and filled among GNP with micro dimensions. Thus, GNP absorbs the molecules of CNTs

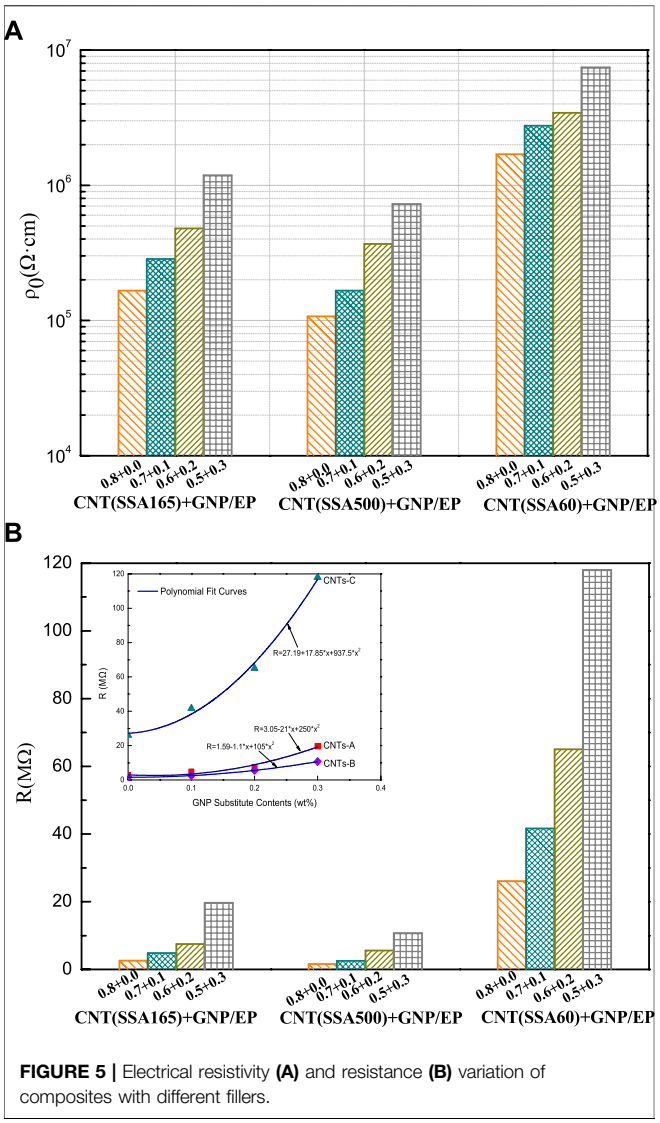

FIGURE 5 | Electrical resistivity **(A)** and resistance **(B)** variation of composites with different fillers.

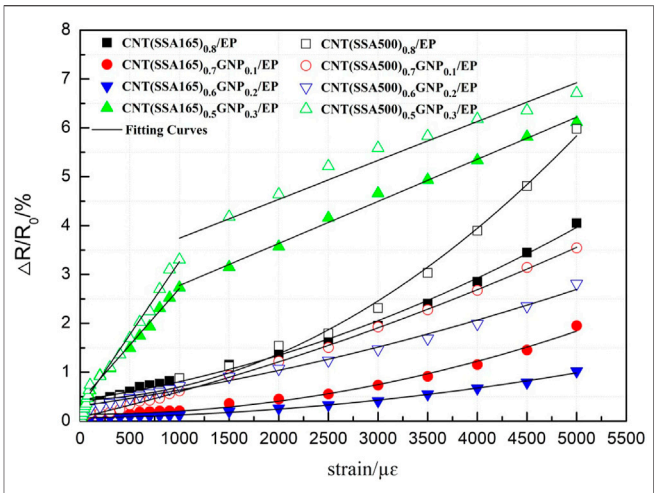

FIGURE 6 | Strain-electrical resistance response peculiarity.

and prevents their aggregations. Moreover, the sandwiched CNTs among the GNP plates bridge the separated plates of GNP from nano scale to micro dimensions, which are expected to further improve the electrical conductivity and sensing sensitivity of the composite. In addition, the approximately oriented conductive network and well dispersed CNTs and GNP fillers in the composites will promote the interaction efficiency and enhance more contact area among carbon fillers and epoxy matrix, which is further expected to lead to better electrical properties, strain-electrical resistance response, and mechanical properties of the composites (Abot et al., 2010; Sengupta et al., 2011; Yang et al., 2020).

By comparing **Figures 4A–C**, it can be found that the SSA of CNTs plays an important role in the dispersion state of CNT-GNP. Composites with CNTs (SSA500) display the most amounts of CNTs and contact points within the same field of vision at the same dosage, seen in **Figures 4B1–B4**. Moreover, the high aspect ratio further resulted in the well-established 3D conductive network. So it is reasonable to conclude that composites with CNT(SSA500) will show the best electrical properties and strain-electrical resistance response peculiarity. On the contrary, composites with CNT(SSA60) appear to have the least CNT conjunction points between the laminar GNP together with the shortest tubular structure. This will lead to the poor electricity conduction, in other words, a much higher dosage of CNT (SSA60) should be required if we want to achieve the same conductivity with other kinds of CNTs.

Electrical and Self-Sensing Peculiarity of the Composites

The electrical resistivity and resistance variation of composites with the SSA change of CNTs and fraction between CNTs and GNP (total filler loading is 0.8 wt%) are displayed in **Figure 5**. The *in situ* electrical resistivity of composites, ρ_0 can be calculated by the formula of $\rho_0 = \frac{R_0 S}{L}$, in which R, S, and L respectively represent the resistance, cross sectional area, and length of the composites specimen. It is clearly seen that composites with CNT(SSA500) display least ρ_0 and R_0 when at the same fraction between CNTs and GNP, which means the optimal electrical conductivity because of the highest SSA and most conductive paths. It is generally believed that the conductivity of CNTs largely depends on the tube diameter and the helix angle of the tube wall (Han et al., 2019). Researchers (Tian et al., 2019) found that CNTs can be regarded as one-dimensional quantum wires with good conductivity when the tube diameter is less than 6 nm, nevertheless, the conductivity of CNTs will decrease when the diameter is larger than 6 nm. On the other hand, ρ_0 and R_0 show a trend of gradual increase with the introduction of GNP when the SSA of CNTs is constant. Furthermore, the growth trend is various for different CNTs, see the small diagram in **Figure 5B**. The increasing data shows exponential growth by fitting, for CNTs-B, $R = 1.59–1.1*x+105x^2$, for CNTs-C, $R = 27.19 + 17.85*x+937.5\ x^2$.

This is related to the lower electrical conductivity of GNP comparing to CNTs. It is worth noting that composites with

TABLE 3 | The fitting parameters of three stages for composites with $CNT(SSA165)_{0.5}GNP_{0.3}$ and $CNT(SSA500)_{0.5}GNP_{0.3}$.

	$CNT(SSA165)_{0.5}GNP_{0.3}$/EP	$CNT(SSA500)_{0.5}GNP_{0.3}$/EP
Stage 1(0 < *x* < 200 με)	$\triangle R/R_0$ = -0.005 + 6.04E-3×strain	$\triangle R/R_0$ = -0.034 + 7.23E-3×strain
Stage 2(200 < *x* < 1000 με)	$\triangle R/R_0$ = 0.401 + 2.31E-3×strain	$\triangle R/R_0$ = 0.275 + 2.99E-3×strain
Stage 3(1000 < *x* < 5000με)	$\triangle R/R_0$ = 1.913 + 8.61E-4×strain	$\triangle R/R_0$ = 2.947 + 7.96E-4×strain

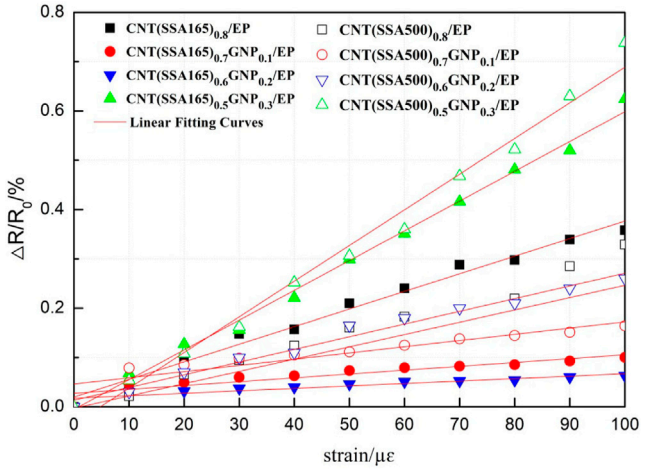

FIGURE 7 | Strain-electrical resistance response peculiarity at strain range of 0-100 με

CNT(SSA60) are shown to be much higher and more unstable R_0 than composites with CNT(SSA165) and CNT(SSA500), so the composites with CNT (SSA60) will not be considered in the following discussions of strain-electrical resistance response peculiarity.

The electrical resistance variation of composites with different CNTs and GNP as the quasi-static tensile loading were recorded in real-time by the self-developed test system. The *in situ* electrical resistance response peculiarity as a function of strain is depicted in **Figure 6**, in which the solid dot represents composites with CNT(SSA165) and the hollow dot represents composites with CNT(SSA500). It is clearly seen that the resistance change rate $\triangle R/R_0$ of all the epoxy composites shows an increasing trend as the increment of tensile within the tested strain range, indicating good self-sensing property. The increase patterns of $\triangle R/R_0$ as strain were remarkably different. For pure CNTs and GNT substituting CNTs by 0.1 wt% and 0.2 wt%, the resistance change rate $\triangle R/R_0$ of epoxy composites displays a trend of linear growth at small strain (less than 1000 με) followed by exponential growth at high elongation strain. Nevertheless, when the substitution of CNT by GNP reaches up to 0.3 wt %, $\triangle R/R_0$ of epoxy composites shows three linear stages with various growth slopes. The slope was highest within the initial strain range (less than 100 με), implying the most sensitivity of strain sensing and ideal monitoring accuracy for asphalt pavement. As the strain increases, the value of the slope drops in the second and third stages. To depict these variations quantitatively, the curves were fitted by piecewise function. The fitting results of the three stages are presented in **Table 3**.

Considering the small structure deformation in asphalt pavement, more emphasis is put on the strain-electrical resistance response peculiarity of the developed composites at micro strain range of 0-100 με. The variations of $\triangle R/R_0$ with strain are presented in **Figure 7**. Apparently, the $\triangle R/R_0$ has a linear relationship with the applied strain. These linear relationships between $\triangle R/R_0$ and strain provide the core foundation for our research and development of sensors. Furthermore, the absolute value of slope increases with the increase of GNP substitution dosage. In this case, the internal structure of conductive domains consisting of CNTs and GNP are difficult to deform at such a small micro strain in the effect of intense connection with the epoxy matrix and codependence between the CNTs and GNP (Spitalsky et al., 2010; Chung, 2019). Deformation is transmitted to the conductive structure through the matrix material when the external force is applied to the composites, which results in less contact among conductive domains and thus the significant increment of resistance. Once the deformation occurs, the conductive domains will separate and have less contact with each other. The corresponding results are the evident increase of resistance. The changes of resistance become more obvious with the increase of GNP, since more GNP in conductive domains will lead to the more diminished contact under tensile. That is why sensing sensitivity improves as the substituting GNP increases.

Besides the synergy effect of CNTs and GNP, the substitutability effect of GNP with CNTs in epoxy composites for asphalt pavement strain monitoring is also focused on for consideration in this study, which can be further explained by the schematic diagram of conducting network structure, see **Figure 8**. To overcome the drawback of the aggregation tendency of CNTs and GNP, the combined advantage is made full use of to further improve the electricity conduction capacity of composites. However, whether there is a better critical substitution between the two carbon fillers is a significant issue. In order to gain an insight into the general tendency of electrical and mechanical properties to change with dosage variation between the two fillers, increasing GNP contents and correspondingly reducing the same CNTs contents are designed with the total filler content which remains fixed. Combining with the comparation of the longitudinal SEM images, it can be observed that the GNP proportion in the total conductive system is increasing from the top to the bottom (see **Figure 4**), corresponding to the decreasing CNTs proportion. However, even though the amounts of CNTs between the adjacent GNP reduce distinctly, the conductivity of CNTs-GNP/epoxy composites will not be lead to a sharp decline

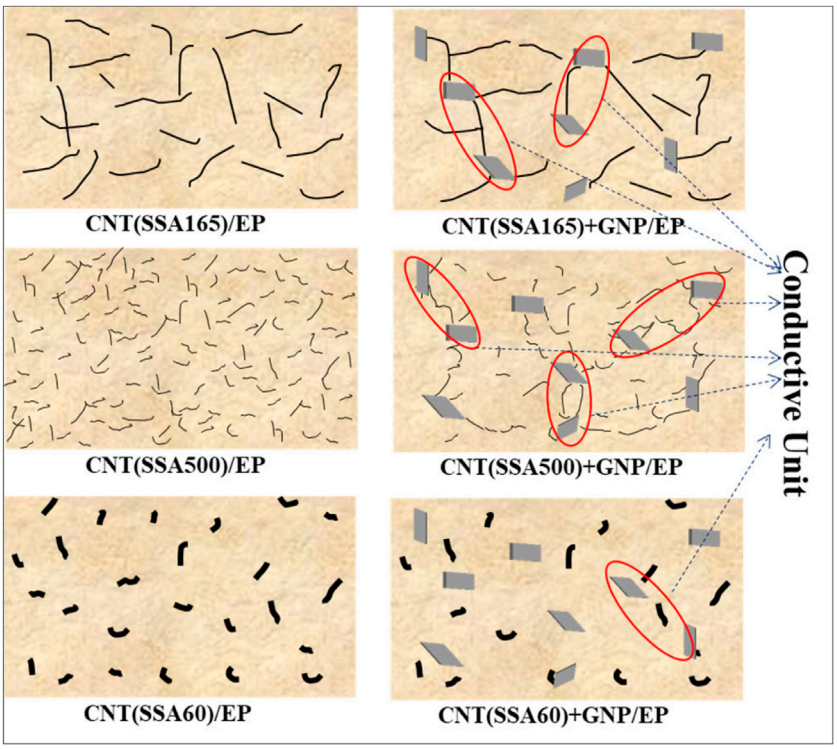

FIGURE 8 | Schematic diagram of conducting network structure.

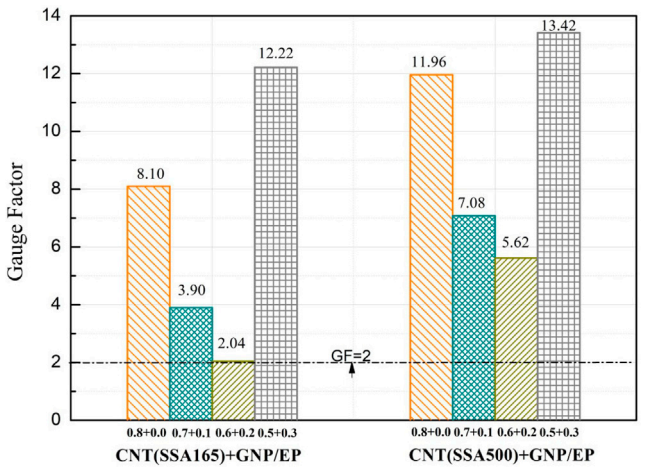

FIGURE 9 | The self-sensing gauge factor of composites under 5000 με.

under the influence of increasing GNP. In the conductive system constituted of GNP and CNTs, the two carbon fillers can prevent aggregation with each other (Ghaleb et al., 2014; Dos Reis et al., 2018; Fang et al., 2020). CNTs dispersed among the GNP and formed conductive units. These conductive units contact with each other and finally construct a three-dimensional conductive network structure. When GNP equivalently replaces the CNT, the amounts of conductive units will increase and the CNTs in each conductive unit will reduce correspondingly. Under the combined influence of the two aspects, the change rate of resistance increases when the external stretch is applied although the conductance decreases slightly.

Furthermore, the $\triangle R/R_0$ of composites with CNT(SSA500) is shown to be obviously higher than that of composites with CNT(SSA165) in the case of composites with CNT(SSA165) and CNT(SSA500) at same filler proportion, which indicates better self-sensing behavior. Comparing to the CNT(SSA165), CNT(SSA500) with smaller out diameter and shorter length presents more numbers of carbon tubes at the same mass fraction. This indicates that more conductive paths will be established in the composites.

In order to gain an insight into the influence of SSA on the sensing sensitivity coefficient, the gauge factor (GF), i.e. sensitivity coefficient, was defined as the following equation, $GF = \frac{\Delta R/R_0}{\varepsilon}$. The calculated GF values are shown in **Figure 9**. It is found that the GF is affected by both CNTs' SSA and GNP substitution dosage. Composites with higher GNP substitution dosage present, first, decreasing and then increasing GF, which is beneficial to the development of self-sensing sensors. Considerable interests have been aroused to explore the potential mechanism for the phenomenon (Bisht et al., 2020). As indicated previously, the strain-electrical resistance response peculiarity of the composites strongly depends on the formed conductive structure and networks. With the increase of GNP substitution dosage, the contents and volume fraction of CNTs reduce correspondingly. The amounts of conductive domains constructed with GNP and CNTs increase in the composites,

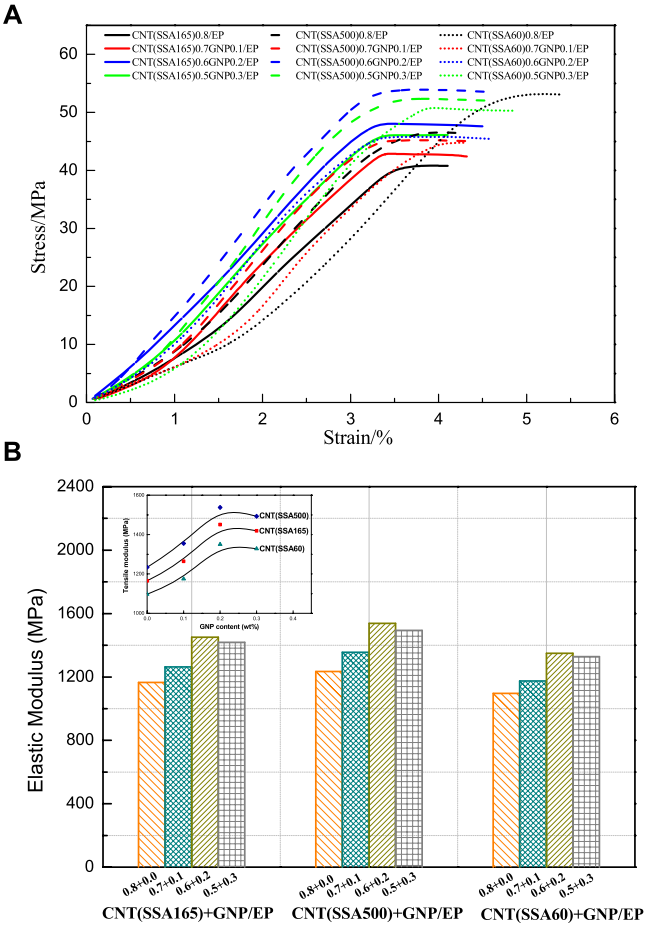

FIGURE 10 | Tensile properties of the epoxy composites with 0.8 wt% carbon fillers. **(A)** strain-stress curves of the composites, **(B)** elasticity modulus of the composites.

despite the quantity of CNTs in each conductive domain dropping off. Just like the conductance of a single copper wire is almost the same as that of unwound multistrand copper wire, the CNTs between the adjacent GNP existing in the form of an independent and dispersed state will present approximate resistance values. However, parts of CNTs among the GNP exist in the interlocking state, which will give rise to the increasing resistance with the combined action of higher GNP substitution dosage. With the gradually increasing applied strain, the deformation transferred to the conductive network structure through the epoxy matrix will be greater due to the micron scale effect of GNP. That is why the higher the GNP substitution dosage, the more obvious the resistance change rate at the same applied strain.

Tensile Properties of the Epoxy Composites

The mechanical properties of the epoxy composites with total 0.8 wt% carbon fillers composed of CNTs and GNP were investigated under quasi-static tensile properties to verify the suitability of the composite modulus for asphalt mixture. **Figure 10** displays the stress-strain curves and the calculated elasticity modulus of all the composites. With the increasing applied stress, all of the composites present approximately linear growth tendency with strain. When the strain reaches a certain value, the stress will remain nearly constant until the breakage of composites, in which the constant stress represents the ultimate tensile strength and the breakup strain represents the maximum tensile strain. The introduced GNP partial substitution of CNTs has brought about a noticeable change to the composites' mechanical behavior. The ultimate tensile strength of the CNTs-GNP reinforced composites is much higher than that of CNTs reinforced composites. This was due to the enhancement of the interface adhesion between CNTs and epoxy matrix after the addition of GNP (Yang et al., 2020). The addition of multilayer GNP promotes the dispersion of CNTs in the epoxy matrix, and the bonding between CNTs and GNP can further inhibit the aggregation and entanglement of CNTs. On the other hand, the CNTs can also restrain the build-up of GNP to avoid re-aggregation with each other. Under the above-mentioned mechanism, CNTs and GNP reinforce the epoxy matrix by the means of the formed three-dimensional network in the matrix. However, composites with GNP substitution dosage of 0.3 wt% are lower than that of 0.2 wt%, which is because of the density difference between CNTs and GNP. The GNP substitution dosage shows the highest value in modulus as the GNP increases.

Figure 10B displays the elastic modulus of composites with different carbon fillers. It is well known that the higher the degree of the load transfer between the monitoring sensor and the detected materials, the monitoring accuracy will be better. So the elastic modulus of the self-sensing composites should be equivalent to that of the asphalt mixture. As shown in **Figure 10B**, although the elastic modulus varies with the different carbon filler, it generally falls within the range of 1100 MPa to 1500 MPa (modulus range of asphalt mixture). The elastic modulus of composites basically overlaps with that of the asphalt mixture, which keeps the same deformation between composites sensor and asphalt mixtures. The collaborative deformation among sensor and asphalt pavement structure ensure the accuracy of the monitoring results.

Sensor Encapsulation and Bending Strain Test in Asphalt Concrete Beam

The most common forming methods of conductive composites include surface conductive film formation method, conductive filler dispersion and cladding method, conductive material lamination method, etc. However, when these methods are used for conducting property tests after the samples are prepared, the conductive glue such as silver adhesive electrode, aluminum foil adhesive electrode, or tin welding method, is generally used to connect wires. Some disadvantages are inescapable, such as the decreased smoothness of the specimen's surface, the long curing time of conductive adhesive, the insufficient bonding effect of conductive adhesive and the unstable contact electrical signal. In order to solve the above problems, we developed the new manufacturing method and the integrated forming mould of composites material with embedded conductive electrode, seen as **Figure 11A**. In the manufacturing device, the conductive wires will be pre-embedded in the mould through the cap plugs at both

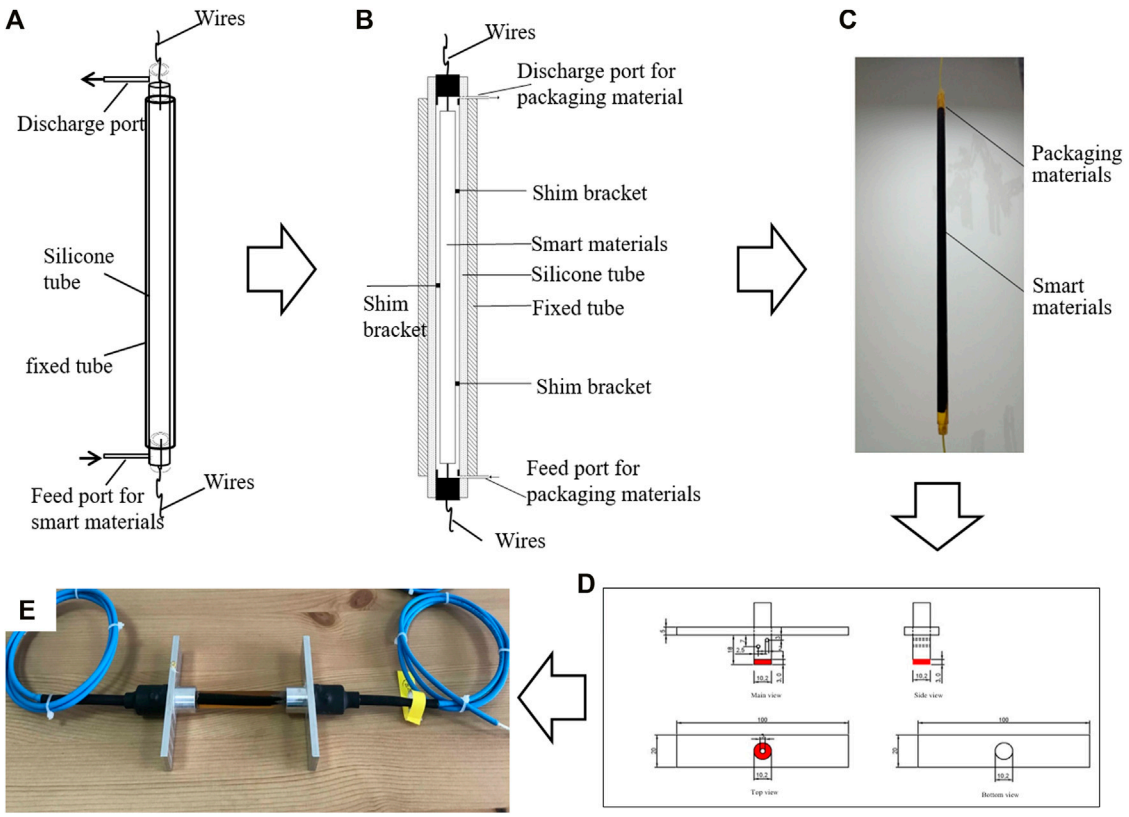

FIGURE 11 | The encapsulation and installation of sensor. **(A)**. Integrated forming mould of composites material with conductive electrode, **(B)**. Encapsulation mould of the sensor, **(C)**. The encapsulated sensor, **(D)**. Schematic diagram of I-beam design, **(E)**. schematic of the installed sensor.

ends of the silicone tube. A feed port and a discharge port are arranged on both sides of the cap plug for the inflow and outflow of composite materials. The fixed acrylic tube with the inner diameter close to the external diameter of the silicone tube is tailored to keep the cured composites vertical. After preparation of the self-sensing composites, the encapsulation mould of the sensor is carried out for the protection of composites, seen as **Figure 11B**. Three semi-circular shaped shim brackets with the inner diameter the same as the self-sensing composites and same thickness as the encapsulated layer are pasted on the composites specimen to ensure composites strip in the center. After the mold is assembled, epoxy resin will be injected as the encapsulated material and the encapsulated sensor is displayed as **Figure 11C**. With the advantage of convenient and easy production and high production efficiency, the developed methods for the sensor's moulding and encapsulation can bring considerable benefits as compared to traditional methods. Afterwards, the aluminum I-beam is designed and installed for the sensors, in order to embed in the asphalt concrete.

To assess the monitoring effectiveness and applicability of the self-sensing composites sensor, the bending strain test was further conducted on the asphalt mixture beam embedded with a developed sensor. The self-sensing composites sensor based of $CNT(SSA500)_{0.5}GNP_{0.3}$/EP was embedded in the bottom of the double-layer plate rutting specimen with the size of 300 mm × 300 mm×100 mm and then AC13 asphalt mixture was compacted in the rutting mould according to the experimental specification (Ministry of Transport, 2011). After 24 h of curing, the rutting specimens were cut into beam with the size of 300 × 100 × 100 mm. The beam with self-sensing composites sensor embedded at the bottom (see **Figure 12B**) was conducted with the three point bending load test (see **Figure 12A**). The three point bending load test was controlled under the program displacement control mode of 0.1 mm/min (see **Figure 12C**). At the same time, three parallel strain gauges with the same length as the self-sensing composites sensor were pasted at the bottom of the beam in order to compare and verify the strain values. During the three point bending load test, the electrical resistance was collected and recorded synchronously (see **Figure 12D** and **Figure 12E**). According to the results of the three-point bending test, the resistance change rate $\triangle R/R_0$ of self-sensing composites sensor also shows the similar increase trend as calibrated by the self-developed test system, except that the increase slope decreased slightly. Through the embedment test in the laboratory, the developed polymer composite sensor displays quite good survival rate under the high temperature and high pressure compacting condition of asphalt mixture. Most importantly, the developed sensor shows high accuracy in strain monitoring for asphalt mixture, even though the asphalt beam underwent very small deformation. The $\triangle R/R_0$ of the self-sensing composite sensor based off $CNT(SSA500)_{0.5}GNP_{0.3}$/EP

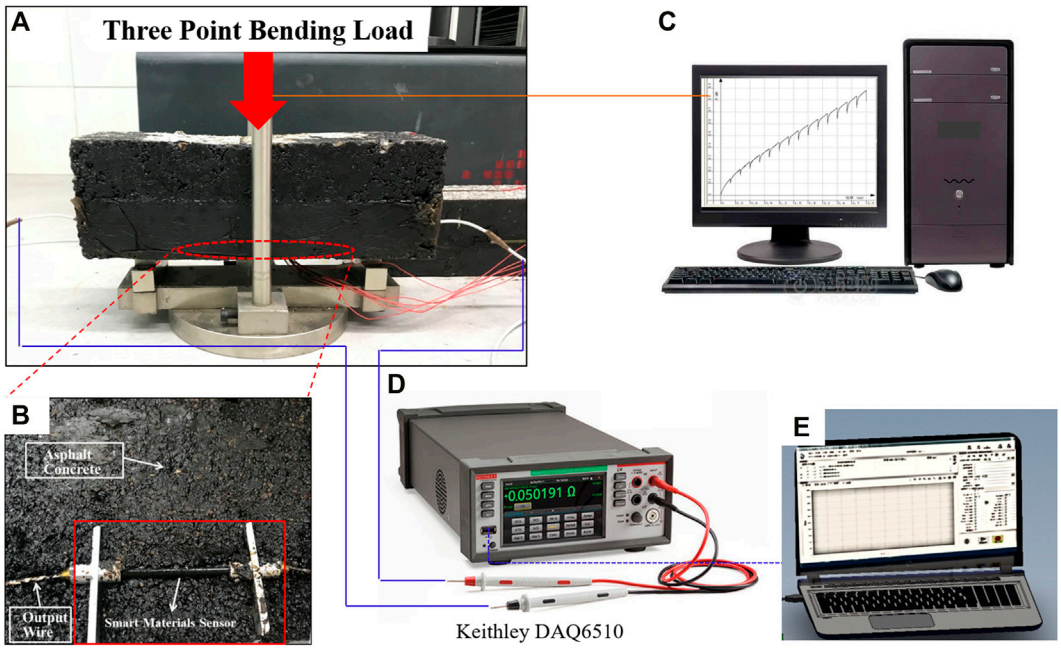

FIGURE 12 | Bending strain test of the self-sensing composites sensor in asphalt concrete beam.

also shows a linear growth trend within 200 με, but the growth slope is 80% of that measured by the laboratory calibration table experiment.

CONCLUSION

The self-sensing strain sensors for asphalt pavement were developed novelly based on the composites with CNT and GNP. The effect of CNTs with different SSA on the CNT-GNP hybrids/epoxy composites were investigated simultaneously. The results showed that CNTs-GNP hybrid in composites presented better dispersion state because of the size effect and synergetic effect comparing to the pure CNTs which were entangled with each other. In the case of CNTs-GNP hybrid conductive structure, CNTs are distributed among the adjacent laminar GNP and the original configuration of pure CNTs or GNP are disrupted and rearranged. Composites with CNT (SSA500) display most amounts of conductive domains within the uniform scale field of vision at same dosage. Moreover, the higher aspect ratio will result in the well-established 3D conductive network. $\triangle R/R_0$ of all the epoxy composites shows an increasing trend as the increment of external tensile in the experimental range, which indicates good self-sensing property. The $\triangle R/R_0$ of composites with CNT (SSA500) is shown to be obviously higher than that of composites with CNT (SSA165), indicating better self-sensing behaviors. CNTs and GNP reinforced the epoxy matrix by forming a three-dimensional network in the matrix. The modulus of composite sensors is in accordance with that of asphalt mixture, which ensures the collaborative deformation among sensor and asphalt pavement structure, and thus the accuracy of monitoring results. Laboratory experiments, by means of a three-point bending test for an asphalt mixture beam-embedded developed polymer composite sensor, verified the durability of the sensor and its high accuracy in strain monitoring for asphalt pavement.

DATA AVAILABILITY STATEMENT

The original contributions presented in the study are included in the article/Supplementary material, further inquiries can be directed to the corresponding authors.

AUTHOR CONTRIBUTIONS

XX: Data curation, Writing - original draft, Writing—review and editing. XL: Methodology. LS: Investigation. ML: Writing–original draft, Writing—review and editing, Funding acquisition. ZY: Project administration, Supervision. CM and XD: Investigation. All authors have read and agreed to the published version of the manuscript. We confirm that the order of authors listed in the manuscript has been approved by all named authors.

FUNDING

The authors acknowledge the financial support of the National Natural Science Foundation of China (No. 51908330), the Qilu Young Scholars Program of Shandong University (No. 202099000060), Natural Science Foundation of Shandong Province (CN) (No. ZR2020ME244) and the Fundamental Research Funds of Shandong University (No. 2020GN059).

REFERENCES

Abdo, M. (2014). *Structural Health Monitoring, History, Applications and Future, A Review Book*. San Francisco: Open Science.

Abot, J. L., Song, Y., Vatsavaya, M. S., Medikonda, S., Kier, Z., Jayasinghe, C., et al. (2010). Delamination Detection with Carbon Nanotube Thread in Self-Sensing Composite Materials. *Composites Sci. Tech.* 70 (7), 1113–1119. doi:10.1016/j.compscitech.2010.02.022

Bisht, A., Dasgupta, K., and Lahiri, D. (2020). Evaluating the Effect of Addition of Nanodiamond on the Synergistic Effect of Graphene-Carbon Nanotube Hybrid on the Mechanical Properties of Epoxy Based Composites. *Polym. Test.* 81, 106274. doi:10.1016/j.polymertesting.2019.106274

Campo, M., Jiménez-Suárez, A., and Ureña, A. (2015). Effect of Type, Percentage and Dispersion Method of Multi-Walled Carbon Nanotubes on Tribological Properties of Epoxy Composites. *Wear* 324-325, 100–108. doi:10.1016/j.wear.2014.12.013

Can-Ortiz, A., Abot, J. L., and Avilés, F. (2019). Electrical Characterization of Carbon-Based Fibers and Their Application for Sensing Relaxation-Induced Piezoresistivity in Polymer Composites. *Carbon* 145, 119–130. doi:10.1016/j.carbon.2018.12.108

Chen, H., Jacobs, O., Wu, W., Rüdiger, G., and Schädel, B. (2007). Effect of Dispersion Method on Tribological Properties of Carbon Nanotube Reinforced Epoxy Resin Composites. *Polym. Test.* 26 (3), 351–360. doi:10.1016/j.polymertesting.2006.11.004

Cheng, H. D., and Miyojim, M. (1998). Novel System for Automatic Pavement Distress Detection. *J. Comput. Civil Eng.* 12 (3), 145–152. doi:10.1061/(asce)0887-3801(1998)12:3(145)

Chung, D. D. L. (2019). A Review of Multifunctional Polymer-Matrix Structural Composites. *Composites B: Eng.* 160, 644–660. doi:10.1016/j.compositesb.2018.12.117

Chung, D. D. L. (2012). Carbon Materials for Structural Self-Sensing, Electromagnetic Shielding and thermal Interfacing. *Carbon* 50 (9), 3342–3353. doi:10.1016/j.carbon.2012.01.031

Dai, H. (2017). An Innovative Sensing Approach Using Carbon Nanotube-Based Somposites for Structural Health Monitoring of concrete Structures. Doctoral Dissertation. Newark, DE(USA): University of Delaware Library.

Dos Reis, J., Oliveira Costa, C., and Sá da Costa, J. (2018). Strain Gauges Debonding Fault Detection for Structural Health Monitoring. *Struct. Control Health Monit.* 25 (12), e2264. doi:10.1002/stc.2264

Escalona-Galvis, L. W., and Venkataraman, S. (2021). Optimum Reduction of Sensing Electrodes for Delamination Identification with Electrical Resistance Tomography. *Struct. Control Health Monit.* 28 (6), e2726. doi:10.1002/stc.2726

Eswaraiah, V., Balasubramaniam, K., and Ramaprabhu, S. (2012). One-pot Synthesis of Conducting Graphene-Polymer Composites and Their Strain Sensing Application. *Nanoscale* 4 (4), 1258–1262. doi:10.1039/c2nr11555g

Fang, Y., Li, L.-Y., and Jang, S.-H. (2020). Calculation of Electrical Conductivity of Self-Sensing Carbon Nanotube Composites. *Composites Part B: Eng.* 199, 108314. doi:10.1016/j.compositesb.2020.108314

Gao, L., Thostenson, E. T., Zhang, Z., and Chou, T.-W. (2009). Coupled Carbon Nanotube Network and Acoustic Emission Monitoring for Sensing of Damage Development in Composites. *Carbon* 47, 1381e1388. doi:10.1016/j.carbon.2009.01.030

Ghaleb, Z. A., Mariatti, M., and Ariff, Z. M. (2014). Properties of Graphene Nanopowder and Multi-Walled Carbon Nanotube-Filled Epoxy Thin-Film Nanocomposites for Electronic Applications: The Effect of Sonication Time and Filler Loading. *Composites A: Appl. Sci. Manufacturing* 58, 77–83. doi:10.1016/j.compositesa.2013.12.002

Han, B., Yu, X., and Kwon, E. (2009). A Self-Sensing Carbon Nanotube/cement Composite for Traffic Monitoring. *Nanotechnology* 20 (44), 445501. doi:10.1088/0957-4484/20/44/445501

Han, S., Meng, Q., Araby, S., Liu, T., and Demiral, M. (2019). Mechanical and Electrical Properties of Graphene and Carbon Nanotube Reinforced Epoxy Adhesives: Experimental and Numerical Analysis. *Composites Part A: Appl. Sci. Manufacturing* 120, 116–126. doi:10.1016/j.compositesa.2019.02.027

Han, S., Meng, Q., Xing, K., Araby, S., Yu, Y., Mouritz, A., et al. (2020). Epoxy/graphene Film for Lifecycle Self-Sensing and Multifunctional Applications. *Composites Sci. Tech.* 198, 108312. doi:10.1016/j.compscitech.2020.108312

Hasni, H., Alavi, A. H., Chatti, K., Lajnef, N., and Lajnef, C. N. (2017). A Self-Powered Surface Sensing Approach for Detection of Bottom-Up Cracking in Asphalt concrete Pavements: Theoretical/numerical Modeling. *Construction Building Mater.* 144, 728–746. doi:10.1016/j.conbuildmat.2017.03.197

Hu, N., Karube, Y., Arai, M., Watanabe, T., Yan, C., Li, Y., et al. (2010). Investigation on Sensitivity of a Polymer/carbon Nanotube Composite Strain Sensor. *Carbon* 48 (3), 680–687. doi:10.1016/j.carbon.2009.10.012

Ko, J. M., and Ni, Y. Q. (2005). Technology Developments in Structural Health Monitoring of Large-Scale Bridges. *Eng. Struct.* 27 (12), 1715e1725. doi:10.1016/j.engstruct.2005.02.021

Koo, G. M., and Tallman, T. N. (2020). Higher-order Resistivity-Strain Relations for Self-Sensing Nanocomposites Subject to General Deformations. *Composites Part B: Eng.* 190, 107907. doi:10.1016/j.compositesb.2020.107907

Kranauskaitė, I., Macutkevič, J., Borisova, A., Martone, A., and Banys, J. (2018). Enhancing Electrical Conductivity of Multiwalled Carbon Nanotube/epoxy Composites by Graphene Nanoplatelets. *Lith. J. Phys.* 57 (4), 232–242. doi:10.3952/physics.v57i4.3602

Ku-Herrera, J. J., Pacheco-Salazar, O. F., Rios-Soberanis, C. R., Dominguez-Rodriguez, G., and Aviles, F. (2016). Self-sensing of Damage Progression in Unidirectional Multiscale Hierarchical Composites Subjected to Cyclic Tensile Loading. *Sensors* 16, 400e412. doi:10.3390/s16030400

Li, W., Dichiara, A., and Bai, J. (2013). Carbon Nanotube-Graphene Nanoplatelet Hybrids as High-Performance Multifunctional Reinforcements in Epoxy Composites. *Composites Sci. Tech.* 74, 221–227. doi:10.1016/j.compscitech.2012.11.015

Li, W., He, D., and Bai, J. (2013). The Influence of Nano/micro Hybrid Structure on the Mechanical and Self-Sensing Properties of Carbon Nanotube-Microparticle Reinforced Epoxy Matrix Composite. *Composites Part A: Appl. Sci. Manufacturing* 54, 28–36. doi:10.1016/j.compositesa.2013.07.002

Li, Y., Liao, Y., and Su, Z. (2018). Graphene-functionalized Polymer Composites for Self-Sensing of Ultrasonic Waves: An Initiative towards "Sensor-free" Structural Health Monitoring. *Composites Sci. Tech.* 168, 203–213. doi:10.1016/j.compscitech.2018.09.021

Li, Z., Dharap, P., Nagarajaiah, S., Barrera, E. V., and Kim, J. D. (2004). Carbon Nanotube Film Sensors. *Adv. Mater.* 16 (7), 640–643. doi:10.1002/adma.200306310

Liu, F., Hu, N., Ning, H., Atobe, S., Yan, C., Liu, Y., et al. (2017). Investigation on the Interfacial Mechanical Properties of Hybrid Graphene-Carbon Nanotube/polymer Nanocomposites. *Carbon* 115, 694–700. doi:10.1016/j.carbon.2017.01.039

Liu, J. K., and An, L. (2018). An, Synthesis and Properties of Graphene/carbon Nanotube/epoxy Resin Composites. *Chem. Eng. Trans. (CET Journal)* 71, 949–954. doi:10.3303/CET1871159

Ministry of Transport (2011). *JTG E20-2011, Standard Test Methods of Bitumen and Bituminous Mixtures for Highway Engineering*.

Park, K., Scaccabarozzi, D., Sbarufatti, C., Jimenez-Suarez, A., Ureña, A., Ryu, S., et al. (2020). Coupled Health Monitoring System for CNT-Doped Self-Sensing Composites. *Carbon* 166, 193–204. doi:10.1016/j.carbon.2020.04.060

Sengupta, R., Bhattacharya, M., Bandyopadhyay, S., Bhowmick, A. K., and Bhowmick, A. K. (2011). A Review on the Mechanical and Electrical Properties of Graphite and Modified Graphite Reinforced Polymer Composites. *Prog. Polym. Sci.* 36 (5), 638–670. doi:10.1016/j.progpolymsci.2010.11.003

Sony, S., Laventure, S., and Sadhu, A. (2019). A Literature Review of Next-Generation Smart Sensing Technology in Structural Health Monitoring. *Struct. Control Health Monit.* 26 (3), e2321. doi:10.1002/stc.2321

Soong, T. T., and Cimellaro, G. P. (2009). Future Directions in Structural Control. *Struct. Control. Health Monit.* 16 (1), 7–16. doi:10.1002/stc.291

Spitalsky, Z., Tasis, D., Papagelis, K., and Galiotis, C. (2010). Carbon Nanotube-Polymer Composites: Chemistry, Processing, Mechanical and Electrical Properties. *Prog. Polym. Sci.* 35, 357–401. doi:10.1016/j.progpolymsci.2009.09.003

Sumfleth, J., Buschhorn, S. T., and Schulte, K. (2011). Comparison of Rheological and Electrical Percolation Phenomena in Carbon Black and Carbon Nanotube Filled Epoxy Polymers. *J. Mater. Sci.* 46 (3), 659–669. doi:10.1007/s10853-010-4788-6

Thostenson, E. T., and Chou, T.-W. (2006). Carbon Nanotube Networks: Sensing of Distributed Strain and Damage for Life Prediction and Self Healing. *Adv. Mater.* 18 (21), 2837–2841. doi:10.1002/adma.200600977

Tian, Z., Li, Y., Zheng, J., and Wang, S. (2019). A State-Of-The-Art on Self-Sensing concrete: Materials, Fabrication and Properties. *Composites Part B: Eng.* 177, 107437. doi:10.1016/j.compositesb.2019.107437

Wang, H.-P., Xiang, P., and Jiang, L.-Z. (2020). Optical Fiber Sensing Technology for Full-Scale Condition Monitoring of Pavement Layers. *Road Mater. Pavement Des.* 21 (5), 1258–1273. doi:10.1080/14680629.2018.1547656

Wang, H., Xiang, P., and Jiang, L. (2018). Optical Fiber Sensor Based In-Field Structural Performance Monitoring of Multilayered Asphalt Pavement. *J. Lightwave Technol.* 36 (17), 3624–3632. doi:10.1109/jlt.2018.2838122

Wang, P.-N., Hsieh, T.-H., Chiang, C.-L., and Shen, M.-Y. (2015). Synergetic Effects of Mechanical Properties on Graphene Nanoplatelet and Multiwalled Carbon Nanotube Hybrids Reinforced Epoxy/carbon Fiber Composites. *J. Nanomater.* 2015, 1–9. doi:10.1155/2015/838032

Wei, T., Song, L., Zheng, C., Wang, K., Yan, J., Shao, B., et al. (2010). The Synergy of a Three Filler Combination in the Conductivity of Epoxy Composites. *Mater. Lett.* 64 (21), 2376–2379. doi:10.1016/j.matlet.2010.07.061

Xi, X., and Chung, D. D. L. (2020). Electret Behavior of Carbon Fiber Structural Composites with Carbon and Polymer Matrices, and its Application in Self-Sensing and Self-Powering. *Carbon* 160, 361–389. doi:10.1016/j.carbon.2020.01.035

Xiang, P., and Wang, H. P. (2016). Strain Transfer Analysis of Optical Fiber Based Sensors Embedded in an Asphalt Pavement Structure. *Meas. Sci. Technol.* 27 (7), 075106. doi:10.1088/0957-0233/27/7/075106

Xiang, P., and Wang, H. (2018). Optical Fibre-Based Sensors for Distributed Strain Monitoring of Asphalt Pavements. *Int. J. Pavement Eng.* 19 (9), 842–850. doi:10.1080/10298436.2016.1211872

Xin, X., Liang, M., Yao, Z., Su, L., Zhang, J., Li, P., et al. (2020). Self-sensing Behavior and Mechanical Properties of Carbon Nanotubes/epoxy Resin Composite for Asphalt Pavement Strain Monitoring. *Construction Building Mater.* 257, 119404. doi:10.1016/j.conbuildmat.2020.119404

Xin, X., Rong, Y., Su, L., Qiu, Z., Yang, C., Liang, M., et al. (2022). Dynamic Mechanical and Chemorheology Analysis for the Blended Epoxy System with Polyurethane Modified Resin. *J. Renew. Mater.* 10 (4), 1081–1095. doi:10.32604/jrm.2022.018021

Yang, H., Yuan, L., Yao, X., Zheng, Z., and Fang, D. (2020). Monotonic Strain Sensing Behavior of Self-Assembled Carbon Nanotubes/graphene Silicone Rubber Composites under Cyclic Loading. *Composites Sci. Tech.* 200, 108474. doi:10.1016/j.compscitech.2020.108474

Yang, Q. L., Qian, Y., Fan, Z., Lin, J., Wang, D., Zhong, J., et al. (2021). Exploiting the Synergetic Effects of Graphene and Carbon Nanotubes on the Mechanical Properties of Bitumen Composites. *Carbon* 172 (2021), 402–413. doi:10.1016/j.carbon.2020.10.020

Zakaria, M. R., Abdul Kudus, M. H., Md. Akil, H., and Mohd Thirmizir, M. Z. (2017). Comparative Study of Graphene Nanoparticle and Multiwall Carbon Nanotube Filled Epoxy Nanocomposites Based on Mechanical, thermal and Dielectric Properties. *Composites Part B: Eng.* 119, 57–66. doi:10.1016/j.compositesb.2017.03.023

Conflicts of Interest: Author CM was employed by Shandong HI-SPEED Group. Author XD was employed by Shandong HI-SPEED Jiwei Expressway Co. LTD.

The remaining authors declare that the research was conducted in the absence of any commercial or financial relationships that could be construed as a potential conflict of interest.

Publisher's Note: All claims expressed in this article are solely those of the authors and do not necessarily represent those of their affiliated organizations, or those of the publisher, the editors and the reviewers. Any product that may be evaluated in this article, or claim that may be made by its manufacturer, is not guaranteed or endorsed by the publisher.